

Dynamic Mechanical, Thermal, and Morphological Properties of Silane-Treated Montmorillonite Reinforced Polycarbonate Nanocomposites

W. S. Chow, S. S. Neoh

Polymer Engineering Division, School of Materials and Mineral Resources Engineering, Engineering Campus, Universiti Sains Malaysia, Nibong Tebal, 14300 Penang, Malaysia

Received 24 February 2009; accepted 17 June 2009

DOI 10.1002/app.30977

Published online 19 August 2009 in Wiley InterScience (www.interscience.wiley.com).

ABSTRACT: Three different loading of 3-aminopropyltriethoxysilane (APS) was used to modify the Na-montmorillonite via cation exchange technique. The Na-MMT and silane-treated montmorillonite (STMMT) were melt-compounded with polycarbonate (PC) by using Haake Minilab machine. The PC nanocomposite samples were prepared by using Haake Minijet injection molding technique. The intercalation and exfoliation of the PC/MMT nanocomposites were characterized by using X-ray diffraction (XRD) and transmission electron microscopy (TEM). The thermal properties of the PC nanocomposites were investigated by

using dynamic mechanical analyzer and thermogravimetry analyzer. XRD and TEM results revealed partial intercalation and exfoliation of STMMT in PC matrix. Increase of APS concentration significantly enhanced the storage modulus (E') and improved the thermal stability of PC nanocomposites. © 2009 Wiley Periodicals, Inc. *J Appl Polym Sci* 114: 3967–3975, 2009

Key words: polycarbonates; clay; nanocomposites; thermal properties; mechanical properties

INTRODUCTION

Polycarbonate (PC) is a versatile thermoplastic owing to its high toughness, high strength, good heat distortion temperature, excellent dimensional stability, and good electric insulation characteristic.¹ PC also has the outstanding ballistic impact strength and good optical clarity, which makes it widely used in the transparent engineering application. Montmorillonite (MMT) has been extensively used in the research of polymer/clay nanocomposites because of its environmental friendly and attractive chemical intercalation nature.² A relatively low percentage (e.g., 1–5 wt %) of MMT in the polymer matrix could result into great improvement in mechanical, thermal, and optical properties. It is believed that the significant improvement in the mechanical properties and thermal stability was attributed to the strong interfacial interaction and the high surface area interaction between the clay filler and the polymeric matrix.³

Under natural condition, the MMT is likely to stack among the layer via the Van der Waals forces.

Besides, the hydrophilic nature of the clay could lead to incompatibility with most hydrophobic polymeric materials. Thus, chemical modification on the clay or polymer resin or both had been carried out to enhance the interaction between the clay and the polymer.³ The surface of the MMT is commonly modified via cation exchange technique to expand the basal spacing and compatibilize the layered silicate with most hydrophobic polymer matrix.⁴ Modification of the hydrophilic clay surface was carried out by using silane coupling agent. The silane coupling agent has both hydrophilic end and organophilic end, which enable them to form bonding between the clay layer and the polymeric resin.⁵ According to Dean et al.,⁶ modification of the MMT surface with 3-(acryloxy)propyldimethylmethoxysilane effectively increased the intergallery spacing. These silane-treated clays are able to form intercalation and some exfoliation structure in the urethane acrylate nanocomposite. According to Lu et al.,⁷ polyethylene is grafted with the silane coupling agent for an enhanced compatibility while melt intercalated with the organo-MMT. Ha et al.⁸ also reported that the modification of MMT by using 3-aminopropyltriethoxysilane (APS) shows expansion in the interlayer galleries and hence improved the dispersion of MMT into the epoxy matrix.

Some research works related to PC nanocomposites were reported recently.^{9–13} Yoon et al.⁹ had reported the effect of PC molecular weight and the

Correspondence to: W. S. Chow (chowwenshyang@yahoo.com).

Contract grant sponsor: Universiti Sains Malaysia.

structure of the OMMT on the clay layers dispersion in the PC/OMMT nanocomposites. Huang et al.¹⁰ had demonstrated two methods to prepare PC/MMT nanocomposites. A partially exfoliated structure was obtained via the ring opening polymerization from the cyclic oligomers, whereas the intercalated structures were obtained via melt mixing in a Brabender internal mixer using linear PC. Lee and Han¹¹ had reported the effect of hydrogen bonding on the rheological behaviors of PC/OMMT nanocomposites. The hydroxyl group present on the surface of OMMT is able to form hydrogen bonding with the carbonyl groups of PC. Wu et al.¹² had reported that the epoxy resin compatibilizer could improve the clay dispersion in PC/OMMT nanocomposites. According to Zong et al.,¹³ the PC/acrylonitrile-butadiene-styrene/MMT nanocomposites prepared by using melt intercalation method shows enhancement in thermal stability and lower the flammability whereby the intercalation structure was observed.

The organo-MMT is unstable at high processing temperature. The organo-MMT tends to degrade and form agglomerates on the high processing temperature of PC which is about 220–260°C. Thus, it could suppress the dispersion of the clays in the PC matrix and subsequently weakens the properties of the composites. It is believed that, for achieving a good PC/MMT nanocomposites, two criteria should be met, that is good thermal stability of MMT, and good compatibility between PC and MMT. In other words, the organo-MMT that is compatible with the PC as well as with high thermal stability is required to provide the excellent thermal and mechanical properties for the PC/MMT nanocomposites. Thus, in this work, we attempted to study the effects of silane coupling agent on the thermal and morphological properties of PC/MMT nanocomposites.

EXPERIMENTAL

Materials

The PC resin (Makrolon 2205) was supplied by Bayer Material Science LLC, Pittsburgh, PA. The density of PC is 1.20 g cm⁻³. The MMT was supplied by Southern Clay Products, Texas. The surface area and cation exchange capacity (CEC) of MMT is 750 m² g⁻¹ and 92.6 mequiv/100 g, respectively. APS was used for the chemical modification of MMT. The molecular weight and density of APS is 221.37 g mol⁻¹ and 0.946 g cm⁻³, respectively. Three different excess amounts of APS was used to modify the Na-montmorillonite (NaMMT) and thereafter designated as [silane-treated montmoril-

lonite (STMMT)] STMMT1, STMMT5, and STMMT10.

Silane treatment of MMT

The surface treatment of NaMMT by silane coupling agent was done by deposition from aqueous alcohol. First of all, the silane coupling agent was diluted in the ethanol solution with a concentration of 5.73M (25% ethanol, 75% deionized water) according to the amount calculated in eq. (1). The silane-ethanol solution was stirred by using a mechanical stirrer to prehydrolyze the silane groups into silanol groups. Meanwhile, the NaMMT was stirred separately in ethanol solution for 1 h at 70°C. After the prestirring process, the silane-ethanol solution was mixed with the NaMMT-ethanol solution at room temperature and the solution was left for 20 h stirring for the cation exchange process to take place on the clay surface. This clay modification method is adopted from Dean et al.⁶ The amount of silane required to modify the NaMMT with various concentrations was calculated by using eq. (1) according to Subramani et al.¹⁴

Amount of silane, $X(g)$

$$= \frac{\text{CEC} \times \text{excess amount of silane} \times M_w \text{ of silane}}{\times \text{amount of clay} \times 1000} \quad (1)$$

where CEC = cation exchange capacity.

The NaMMT was modified with various excess amounts of APS (1, 5, and 10) into STMMT1, STMMT5, and STMMT10. Usages of 1.0 excess amount in the clay modification represent the ratio of 1 mol silane coupling agent to 1 mol of the cation charges on the NaMMT. After the modification step, the modified clay was filtered by using vacuum filtration system. The precipitate was then dried in vacuum oven at 100°C for 24 h. The dried fillers were ground into micron size using planetary ball milling and rinsed again with ethanol to remove any possible residual silane before the second drying process took place. The second drying process was carried out at the same temperature and drying period.

Preparation of PC/NaMMT nanocomposites

The PC, Na-MMT, and STMMT were dehumidified in an oven at 100°C for 12 h before compounding. The melt-compounding was carried out by using Haake Minilab (Thermo Electron Corporation). The melt compounding was carried out at 240°C for 15 min in corotating screw mode with a screw speed of 100 rpm. The PC/NaMMT extrudate was pelletized and dried in a vacuum oven at temperature of

TABLE I
Material Designation and Composition of PC Nanocomposites

Sample	Composition (wt %)			APS (excess amount) [Ratio of 1 mol APS to 1 mol of the cation charges on the NaMMT]
	PC	MMT	STMMT	
PCNaMMT3	97	3	–	–
PCSTMMT1	97	–	3	1
PCSTMMT5	97	–	3	5
PCSTMMT10	97	–	3	10

100°C for at least 4 h before the molding process. The PC nanocomposite samples were prepared by using a Haake Minijet (Thermo Electron Corporation) injection molding machine. The cylinder and mold temperature were set at 250°C and 90°C, respectively. PC/STMMT nanocomposites were prepared by 3 wt % loading of STMMT with different concentration of silane coupling agent. Table I shows the material designation and composition of PC nanocomposites.

Sample characterization

Thermogravimetry analysis

Thermogravimetry analysis (TGA) was used to measure the weight changes of the PC nanocomposites sample as a function of temperature. The decomposition temperature and the percentage of decomposition of PC samples were determined by TGA. The TGA was performed using TGA Pyris 1 (PerkinElmer, USA) in nitrogen atmosphere. The sample was weighed in a range of 5–10 mg and heated from 30 to 800°C in a heating rate of 20°C min⁻¹.

Dynamic mechanical thermal analysis

The dynamic mechanical thermal analysis (DMTA) was carried out by using PerkinElmer diamond dynamic mechanical analyzer, model SII exstar 6000. DMTA was used to determine the storage modulus (G'), loss modulus (G''), and tan delta ($\tan \delta$) of the PC nanocomposites samples. The oscillation shear mode was used in a temperature range from -100 to 200°C at the heating rate of 5°C min⁻¹ and 1 Hz frequency for the analysis.

X-ray diffraction

X-ray diffraction (XRD) measurements of the PC nanocomposites were carried out on bars. All these experiments were performed in reflection mode with a D5000 diffractometer (Siemens) using CuK α radiation (wavelength = 0.154 nm) at a scan rate of 1° min⁻¹ in a 2 θ range of 1–10°, and operated at 40 kV

and 30 mA. Bragg's equation is applied to calculate the d -space (d_{001}) for the samples as shown in eq. (2).

$$n\lambda = 2d \sin \theta \quad (2)$$

where n is the number of complete wave ($n = 1$ for d_{001}), λ is the wave length of X-ray used, θ is the reflection angle of X-ray on the silica layer, and d is the distance between silica layer (d_{001}).

Transmission electron microscopy

Transmission electron microscopy (TEM) measurements were carried out with a transmission electron microscope CM12 (Netherlands) operating at an accelerating voltage of 200 kV. The specimens were prepared using a Leica Ultracut UCT ultramicrotome. Ultra-thin sections of about 60 nm in thickness were cut with a diatome diamond knife (35°) at room temperature.

Fourier transform infra-red spectrometry

Fourier transform infra-red spectrometry (FTIR) spectra were recorded by a PerkinElmer Spectrum BXII System 2000 FTIR Spectrometer (France). The predried NaMMT and STMMT were ground with KBr powder in the ratio of 1 : 9 and then compressed into a thin plate shape. A resolution of 2 cm⁻¹ for four scans over wavenumber of 4000–400 cm⁻¹ was performed for the Na-MMT and STMMT.

RESULTS AND DISCUSSIONS

Effects of silane-modification

XRD analysis of silane-modified MMT

Figure 1 shows the XRD patterns of the NaMMT and the modified clay (STMMT) with different silane concentration. The NaMMT, STMMT1, STMMT5, STMMT10 patterns show the characteristic diffraction peaks at $2\theta = 7.77, 5.67, 4.86,$ and $4.67,$ respectively, corresponding to basal spacing (d_{001}) of 1.14, 1.56, 1.82, and 1.89 nm. Interesting to note that, the

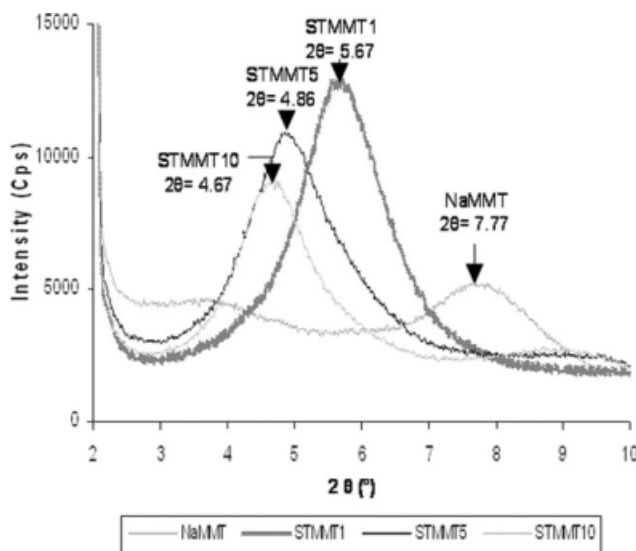


Figure 1 XRD diffractograms of NaMMT and STMMT with various silane concentrations.

d -spacing of the NaMMT was increased significantly by the silane treatment. The d_{001} of NaMMT (1.14 nm) was increased to 1.56 nm in STMMT1. The d_{001} was increased $\sim 37\%$ by using the ratio of 1 mol of silane coupling agent to 1 mol of cation charge on the NaMMT in the clay modification. The higher basal spacing observed for STMMT compared with NaMMT may be attributed to the intercalation of the APS silane coupling agent chain in the intergallery of MMT silicate layers. One may observe that the percentage of increment in the d_{001} was reduced with the increasing concentration of silane coupling agent. The difference of d_{001} increment in STMMT1 and STMMT5 was 0.26 nm, whereas the difference in d -spacing between STMMT5 and STMMT10 was only 0.07 nm. This might be due to the fact that the higher proportion of silane coupling agent saturate the entire surface of the clay. It is believed that the excess amount of silane coupling agent would form intermolecular hydrogen bonds instead of covalent bond to the clay surface, attributed to the affinity and interaction between APS coupling agent and the MMT.

The peaks obtained in silane-modified clays (STMMT) were shifted to a lower 2θ value as the concentration of the silane in the modified clays (STMMT) was increased. This indicates that the APS coupling agent is able to expand the d_{001} of the clay. According to Subramani et al.,¹⁴ there were two mechanisms of the NaMMT modification by using APS: (i) formation of covalent bonds via condensation step and (ii) exchange of the sodium ion present in the galleries of the clay. Thus, it is suggested that the usages of APS in the clay modification is able to increase the distance of the clay layers via the formation of covalent bonds on the clay surface and the ionic bonds in the clay layers.

FTIR analysis of silane-modified MMT

Figure 2 shows the FTIR spectrums of the pristine clay (NaMMT) and silane-modified clays (i.e., STMMT1, STMMT5, and STMMT10). The broad peak at 3447 cm^{-1} refers to $-\text{OH}$ stretching frequency indicating the presence of entrapped water in the interlayer galleries of pristine clay (NaMMT). The peak at 1046 cm^{-1} indicates the $\text{Si}-\text{O}-\text{Si}$ stretching while the peak observed at 916 cm^{-1} is assigned to the $\text{Si}-\text{O}$ stretching vibration. Spectrum peaks at the range of 400 and 800 cm^{-1} could be related to the presence of metallic elements in the pristine clay. For example, the peak at range of 400 and 550 cm^{-1} is attributed to the $\text{Al}-\text{O}$ vibration. From Figure 2 (Region A), a peak found in the range of $3625\text{--}3631\text{ cm}^{-1}$ in both pristine clay (NaMMT) and silane-modified clays (STMMT). This peak is referring to the typical $-\text{OH}$ stretching in the structure. The percentage of transmittance ($T\%$) in this peak was increased with the concentration of APS in the STMMT. The increment in the transmittance ($T\%$) indicates that the amount of $-\text{OH}$ group bonded to the clay surface was increased. This is due to condensation between APS and the clay surface. It is believed that, as the concentration of APS linked to the clay surface is increased, the amount of hydroxyl group present will be increased.

The peaks present in the range of $3446\text{--}3450\text{ cm}^{-1}$ shown in region (B) and $1635\text{--}1638\text{ cm}^{-1}$ in region (D) could be assigned to the adsorbed water molecules. The transmittance of the water peak is decreasing with the increasing of APS concentration. The silanols were bonded to the interlayer of the silicates via condensation.¹⁴ The H_2O released in the condensation step was removed in the precipitate washing followed by the drying steps. Thus, the amount of the water present in the interlayer is reduced with the increasing of APS concentration.

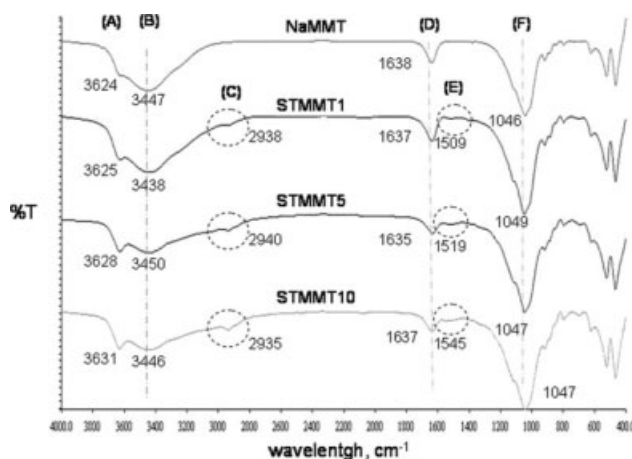


Figure 2 FTIR spectrums of NaMMT and STMMT with various silane concentrations.

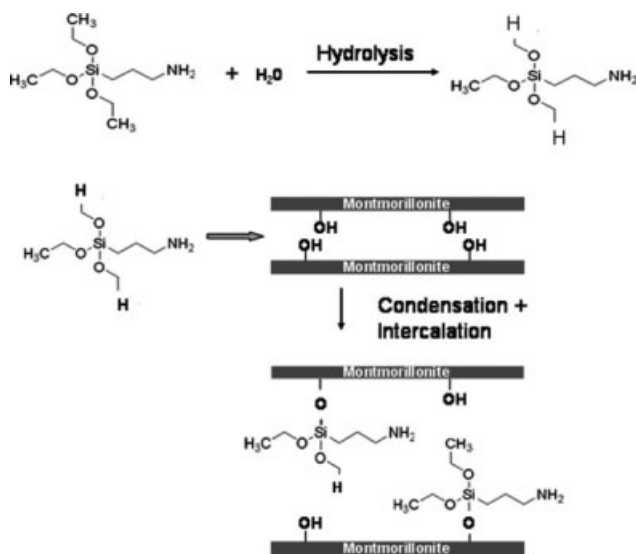


Figure 3 Possible reaction between APS and MMT.

As shown in region (C), there are new peaks at range of $2800\text{--}3000\text{ cm}^{-1}$ observed in silane-modified clays (STMMT) compared with that of the pristine clays (NaMMT). This new band is due to the —CH asymmetric and symmetric stretching of —CH_2 groups.¹⁵ Those peaks confirmed the presence of APS on the clay surface. Besides, a peak observed at range of 1509 and 1545 cm^{-1} is due to the N—H bending in the structure. Referring to region (E), only modified clay (STMMT) show the peak in this range. This result indicates the present of amine functional groups in APS was bonded to the clay surface after the silane modification process. Refer to region (F) it can be observed that, some peaks were shown at the range of $1046\text{--}1049\text{ cm}^{-1}$ in both pristine clay (NaMMT) and silane-modified clays (STMMT). Those peaks with this range of wavenumber could be related to the Si—O stretching vibration in the structure. Figure 3 shows the possible reaction between APS and MMT. It is believed that the APS could intercalate into the MMT silicate layers and further form chemical bonds with the MMT.

TGA of silane-treated MMT

Figure 4 shows the TGA curves of pristine clay (NaMMT) and the silane-treated clays (STMMT). The onset temperatures of the clays were tabulated in Table II. The first region (T_{onset1}) was the decomposition of free water which occurred below 100°C . This initial mass loss was dominated by free water trapped on the clay surface and interlayer galleries in both unmodified (NaMMT) and modified clays (STMMT). The release of free water in NaMMT began around 68°C while the loss of free water in STMMT occurred around 40°C . According to Xie

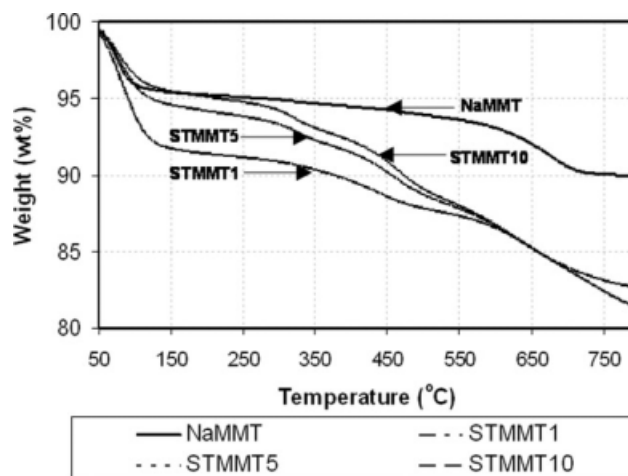


Figure 4 TGA curves of STMMT with various silane concentrations.

et al.,¹⁵ there were numerous environments of water in the MMT. Weakly bound, physioadsorbed water, and free water pockets within the aggregate structure evolve at the lowest temperature, whereas water within the interlayer and strongly bonded water of hydration (Na^+) evolve at progressively higher temperatures.

The second region (T_{onset2}) and third region (T_{onset3}) observed in the TGA curves were related to the decomposition of the organosilyl groups in the STMMT. The T_{onset2} is occurring between 250 and 350°C whereas the T_{onset3} is between 400 and 500°C . According to Herrera et al.¹⁶ and Park et al.,¹⁷ there are three possibility sites that the functionalization of clay mineral can take place: (i) at the interlayer space, (ii) at the external surface, and (iii) at the edges of the clay. During the modification, the silanol group interacts with the hydroxyl group from the clay surface via hydrogen bonds which condensed to form covalent bonds among APS and clay surface.⁷ The decomposition occurred at the third region is due to the loss of the organosilyl groups which were covalently bonded to the surface of the clay.¹⁸ This type of modification provides higher thermal stability due to the high stability of covalent bond.

TABLE II
Onset Temperature (T_{onset}) of NaMMT and STMMT with Various Silane Concentrations

Sample	T_{onset1} ($^\circ\text{C}$)	T_{onset2} ($^\circ\text{C}$)	T_{onset3} ($^\circ\text{C}$)	T_{onset4} ($^\circ\text{C}$)
NaMMT	67.9	—	—	673.0
STMMT1	40.4	—	361.9	590.0
STMMT5	41.5	269.6	414.8	595.1
STMMT10	39.0	296.4	412.8	567.0

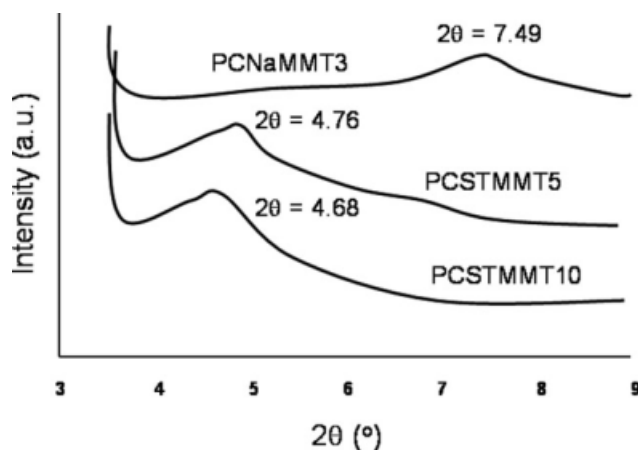


Figure 5 XRD diffractograms of PCNaMMT3, PCSTMMT5, and PCSTMMT10.

STMMT1 do not show the decomposition step in the range of second region. While the STMMT5 and STMMT10 show increase in the mass loss with the concentration of APS coupling agent used. One of the possibilities for the observation is due to the formation of chain extension in the silanols via hydrogen bonds with the neighbor atoms.^{6,14} It is believed that the possibility of the chain extension increases with the increasing loading of APS concentration. The fourth region in the TGA thermal analysis occurred in the range of 550–800°C in NaMMT and STMMT were associated to the dehydration of structural water from the clay. Similar observation was reported by Subramani et al.¹⁴ In addition, one may found that the amount of residue remained at 750°C are 90% for NaMMT and 82–83% for STMMT. This can be related to the MMT ash content after the decomposition at high temperature. Noteworthy that with silane modification this residue remains unaltered in STMMT regardless of the amount of APS content.

Properties of PC nanocomposites

XRD analysis of PC/MMT nanocomposites

Figure 5 shows the XRD patterns (in the range of $2\theta = 2\text{--}10^\circ$) of PCSTMMT5 and PCSTMMT10 nanocomposites. The corresponding d -spacing values of PCNaMMT3, PCSTMMT5, and PCSTMMT10 are 1.18, 1.85, and 1.89 nm, respectively. One may observe that the d_{001} of PC/clay nanocomposites was increased by the STMMT. It can be seen that the 2θ of the PC/MMT was shifted to a lower angle by the silane modification. For PCSTMMT10, a broad shoulder peak at $2\theta = 4.68^\circ$ appeared in the XRD pattern might be due to partial exfoliation of the modified clay in the nanocomposites. Note that the d -spacing of PCSTMMT5 (1.85 nm) is higher than that of PCNaMMT3 (1.18 nm). This indicates that

the distance of the interlayer is increased in the presence of APS coupling agent. This could be related to the intercalation and exfoliation of the MMT layer silicates by the silane-modification. The intensity of d_{001} characteristic peaks of PC/clay nanocomposites was reduced by the silane-modification. Reduction of the intensity might due to partially exfoliation of the modified clay or the concentration of clay in the diffraction specimen.¹¹

Morphological properties of PC/MMT nanocomposites

The TEM photographs of PCNaMMT3 and PCSTMMT10 were displayed in Figures 6 and 7. The dark lines represent the thickness of individual clay layers or clay agglomerates. The darker lines show stacked silicate layers due to clustering of agglomerates (tactoids). From Figure 6, it can be seen that the unexfoliated and agglomerated NaMMT particle was observed on the PCNaMMT3. Figure 7(a,b) shows the morphology of PCSTMMT10 at high magnification. Shear induced silicate layers intercalation is observed in Figure 7(a) where the single layer of the silicate was shear from the layered structure in pristine clay. The average thickness of the clay platelets appears to be ~ 15 nm, whereas the average length is about 100 nm. This is attributed to the high shearing during the extrusion process. The layered silicate of MMT was sheared and delaminated into thinner silicate layer upon subjected to melt shearing. From Figure 7(b), it can be observed that the silane-modified clay is partially intercalated and exfoliated in the PC matrix. This is consistent with the XRD results. Recall that the hydrolyzed APS was interacting with the clay surface due to the hydrogen bonds between the oxide surfaces of clay and silanol group in APS. The long propyl chains in the APS were

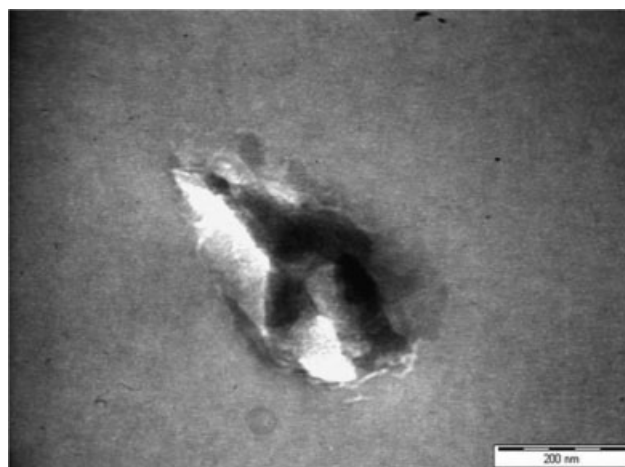


Figure 6 TEM photograph taken from the PCNaMMT3 nanocomposites.

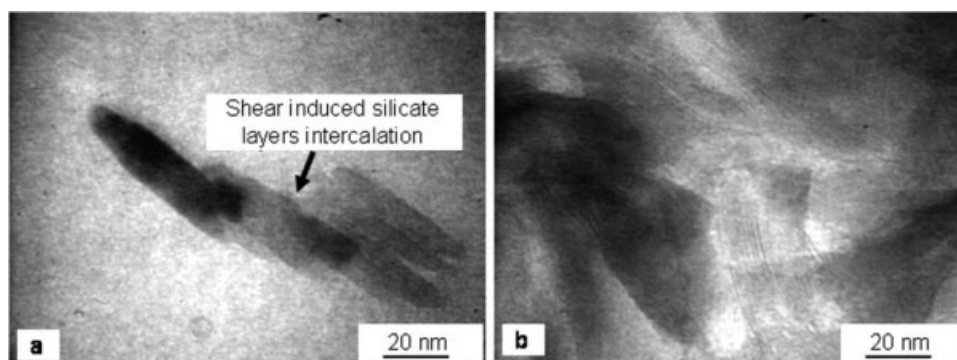


Figure 7 TEM photomicrograph taken from PCSTMMT10 nanocomposites: (a) Shear induced silicate layers intercalation and (b) exfoliation and intercalation of silicate layers.

then increased the d -spacing of the NaMMT layered silicates. From the XRD, it was found that the d -spacing of STMMT10 was increased about 0.75 nm compared with that of the pristine clay (NaMMT). The PC chains were intercalated into the interlayer galleries easily with the higher d -spacing which was expanded by the silane coupling agent. The hydrophilic end of the APS is linked to the surface of clay while the organo-functional end of the silane coupling agent is likely to interact with PC resins. According to Di Gianni et al.,¹⁸ the interaction between the silane coupling agent with the polymer resins able to intercalate the polymer chains into the silicate galleries.

Thermal properties of PC/MMT nanocomposites

Figure 8 reveals the TGA curves recorded from PCNaMMT3, PCSTMMT1, PCSTMMT5, and PCSTMMT10. The onset temperature (T_{onset}) of the materials decomposition was summarized in Table III.

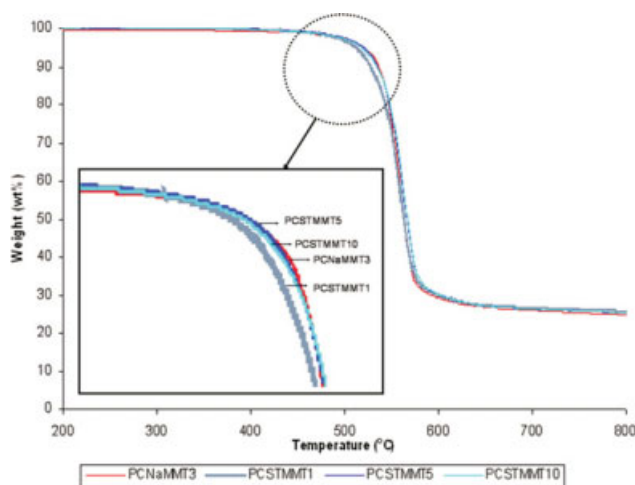


Figure 8 TGA curves of PCNaMMT3 and PCSTMMT with various silane concentrations. [Color figure can be viewed in the online issue, which is available at www.interscience.wiley.com.]

Note that the degradation for all the nanocomposites happened after 530°C. As seen from Figure 8, the thermal stability of PCSTMMT10 nanocomposites is slightly higher than the PCNaMMT3. The T_{onset} of PCSTMMT10 and PCNaMMT3 is 537.2°C and 533.5°C, respectively. The result indicates that APS was effectively interacting with the PC resins and the clay, and subsequently enhancing the thermal stability of PC/STMMT. This is maybe due to the formation of the crosslinked structure between APS and clay which delay the degradation. According to McCormick et al.,¹⁹ at high temperature, the polymer hydroperoxides are initially generated due to the oxidation mechanism and then combined with pendant silane grafts via a hydrogen bond, rearranged to form silanol and finally these silanols are coupled with each other to form crosslinking. The formation of the crosslinked structure makes the degradation more difficult. It is believed that the modification of NaMMT using silane plays an important role toward the interfacial interaction and compatibility between PC and clay. The improvement in thermal-oxidative stability is mainly attributed to the chemical bonds formed between the polymer matrix and the clay.

Figure 9 shows the storage modulus (E') as a function of temperature for PC/STMMT with various silane concentrations. Table III display the storage modulus (E') of PC/STMMT with various silane concentrations at 30°C. It can be seen that all the

TABLE III
Onset Temperature (T_{onset}), Storage Modulus (G') at 30°C and $\tan \delta$ of PCNaMMT3 with Various Silane Concentrations

Sample	T_{onset} (°C)	Storage modulus, G' at 30°C (MPa)	$\tan \delta$
PCNaMMT3	533.5	715.48	146.04
PCSTMMT1	532.5	824.06	145.46
PCSTMMT5	534.3	836.43	146.04
PCSTMMT10	537.2	816.77	146.02

PC/STMMT nanocomposites exhibited higher value in storage modulus than PCNaMMT over the temperature range examined. As seen in Table III, the storage modulus of PCNaMMT3 (715.5 MPa) has been increased to 836.4 MPa by the silane-modified NaMMT (PCSTMMT5). This indicates that the addition of APS-modified NaMMT significantly increased the storage modulus of PC matrix. This improvement could be associated to the stiffness of the STMMT, the constraining effects of these layers on molecular motion of polymer chains, the high aspect ratio and degree of dispersion of STMMT. According to Lee and Han,¹¹ the increment in the storage modulus value is attributed to the higher aspect ratio of the NaMMT in the nanocomposites. In addition, it is believed that modifying NaMMT by using APS is able to increase the distance of the clay layer, and hence provide larger space for the PC chains intercalation into the clay galleries. The improvement of E' could be correlated to better intercalation and exfoliation of STMMT in PC matrix. In highly intercalated and exfoliated nanocomposites, individual clay layer with high aspect ratio are dispersed homogeneously in polymer matrix. However, increasing in the APS concentration do not shows significant variation in the storage modulus. The result indicates that the stiffness of the nanocomposite was contributed by the clay loading instead of the concentration of the modifier. According to Bao and Tjong,²⁰ the stiffness of nanocomposites was controlled by the increasing loading of the clay filler instead of the effect of the compatibilizer. Table III shows the $\tan \delta$ value of PCNaMMT3 and PC/STMMT with various APS concentrations. The dynamic relaxation peaks was observed at around 145°C. This is assigned to the glass transition temperature (T_g) of the PC. From the results, the T_g peak positions vary slightly in the PC nanocomposites which are in the range of 145.5 and

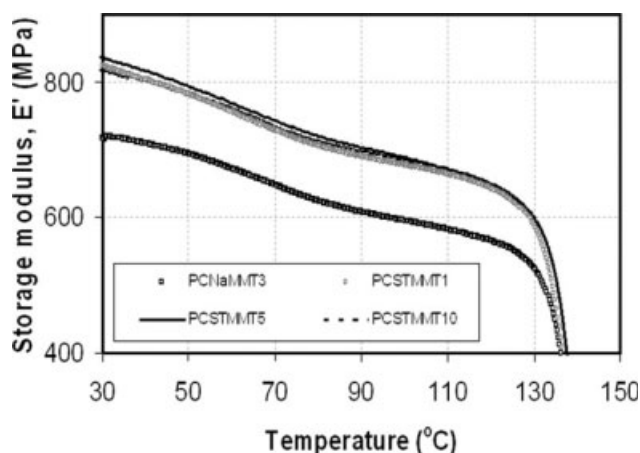


Figure 9 Storage modulus (E') of PCNaMMT3 and PCSTMMT with various silane concentrations.

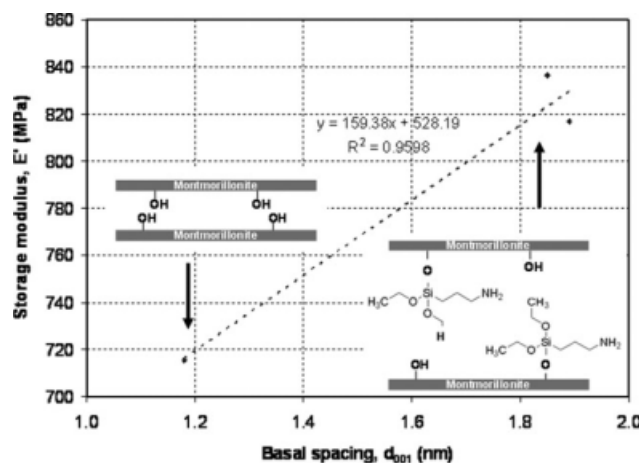


Figure 10 Relationship between basal spacing intercalation and storage modulus.

146.1°C (cf. Table III). This may indicate that the T_g of PC is not affected significantly by the silane coupling agent concentration. Figure 10 shows the relationship between the interlayer basal spacing of MMT (detected from XRD) and storage modulus (recorded from DMTA at 30°C). It can be found that the storage modulus of PC is controlled by the intercalation of MMT. It is worthy to note that storage modulus of PC nanocomposites was increased significantly by the incorporation of STMMT, owing to the fact that the basal spacing of STMMT is higher than that of NaMMT.

CONCLUSIONS

Based on this work devoted to study the effects of STMMT on the thermal and morphological properties of PC nanocomposites, it can be concluded that the PC/STMMT nanocomposites exhibited higher storage modulus and thermal stability compared with that of PC/NaMMT. The enhancement in storage and thermal stability is contributed by the silane coupling agent. In addition, the STMMT is partly intercalated (based on XRD) and partly exfoliated (shown by TEM) in the PC matrices. It is believed that the silane coupling agent could favor the intercalation and exfoliation of MMT in PC.

The authors thank Dr. Pun (Texchem Polymer (M) Sdn Bhd) for materials supply and technical support.

References

- Legrand, G. D.; Bendler, J. T. *Handbook of Polycarbonate Science and Technology*; Marcel Dekker: USA, 2000; Vol. 143.
- Yalcin, B.; Cakmak, M. *Polymer* 2004, 45, 6623.
- Leszczyńska, A.; Njuguna, J.; Pielichowski, K.; Banerjee, J. R. *Thermochim Acta* 2007, 453, 75.

4. Zanetti, M.; Lomakin, S.; Camino, G. *Macromol Mater Eng* 2000, 279, 1.
5. Mark, H. F. *Encyclopedia of Polymer Science and Technology*; Wiley: USA, 2003; Vol. 3.
6. Dean, K. M.; Bateman, S. A.; Simons, R. *Polymer* 2007, 48, 2231.
7. Lu, H.; Hu, Y.; Li, M.; Chen, Z.; Fan, W. *Compos Sci Technol* 2006, 66, 3035.
8. Ha, S. R.; Rhee, K. Y.; Kim, H. C.; Kim, J. T. *Colloids Surf A* 2008, 313–314, 112.
9. Yoon, P. J.; Hunter, D. L.; Paul, D. R. *Polymer* 2003, 44, 5323.
10. Huang, X.; Lewis, S.; Brittain, W. J.; Vaia, R. A. *Macromolecules* 2000, 33, 2000.
11. Lee, K. M.; Han, C. D. *Polymer* 2003, 44, 4573.
12. Wu, D.; Wu, L.; Zhang, M.; Wu, L. *Eur Polym J* 2007, 43, 1635.
13. Zong, R.; Hu, Y.; Wang, S.; Song, L. *Polym Degrad Stab* 2004, 83, 423.
14. Subramani, S.; Choi, S.; Lee, J.; Kim, J. H. *Polymer* 2007, 48, 4691.
15. Xie, W.; Gao, Z.; Liu, K.; Pan, W.; Vaia, R.; Hunter, D.; Singh, A. *Thermochim Acta* 2001, 367, 339.
16. Herrera, N. N.; Letoffe, J.; Putaux, J.; David, L.; Bourgeat-Lami, E. *Langmuir* 2004, 20, 1564.
17. Park, Y.; Lee, D.; Kim, S. *J Appl Polym Sci* 2004, 91, 1774.
18. Di Gianni, A.; Amerio, E.; Monticelli, O.; Bongiovanni, R. *Appl Clay Sci* 2008, 42, 116.
19. McCormick, J. A.; Royer, J. R.; Hwang, C. R.; Khan, S. A. *J Polym Sci B: Polym Phys* 2000, 38, 2468.
20. Bao, S. P.; Tjong, S. C. *Compos A: Appl Sci Manuf* 2007, 38, 378.